Design and Simulation of an Autonomous Smart Microgrid for Energy Independence

HAI N. HO, TONY BUI, HAU DO, ELIUD ROJAS, OMAR OJEDA, HIEN TRAN,
TOMMY HOANG, EDWIN HERNANDEZ, LOC NGUYEN, HA THU LE

Department of Electrical and Computer Engineering
California State Polytechnic University, Pomona
Pomona city, California 91768
UNITED STATES OF AMERICA

Abstract – The project designs a microgrid based on downtown community of El Monte city, California. The system main components include a solar PV system, a battery, a diesel generator, an inverter, a control system, and loads. The microgrid design is simulated using MATLAB Simulink. The results show that the microgrid can supply power to its community adequately and independently without relying on a utility power grid. The microgrid is smart as it can operate autonomously thanks to its automatic control system. For various operational scenarios, the microgrid proves to be resilient where it can supply its load demand successfully using its solar system, battery, and diesel generator. The load voltage is kept at satisfactory values of around 1.0 per unit. The power distribution efficiency is around 99%. The results contribute to development of smart microgrids which, in turn, improve the reliability and resiliency of large power grids, as well as provide energy independence to communities.

Keywords – Battery, diesel generator, inverter, microgrid, solar photovoltaic, smart grid, state flow.

Received: July 20, 2021. Revised: August 17, 2021. Accepted: August 20, 2021. Published: August 23, 2021.

1. Introduction

Thanks to fast development of measurement techniques, intelligent control, and modern communication systems, grid technology has made many advancements in developing smart power systems. The core components of the smart power systems are microgrids. A microgrid is a small integrated energy system consisting of distributed energy resources (DER), energy storage, loads, and a control system. A microgrid can operate synchronously with a wide-area grid or autonomously without the large grid. Microgrids provide significant benefits, such as improving power supply reliability, reducing power losses, providing energy independence to communities, and supporting the use of renewable energy sources, such as solar and wind energy. Hybrid small power systems using solar PV, wind turbine and/or battery have been investigated for various purposes, such as achieving energy independence for family houses and smart farming [1-3]. However, design and functions of microgrids are very diverse and require further exploration. This project investigates a design of a smart microgrid that can operate

autonomously to achieve energy independence for the community that it serves. The following section provides a brief review of key features of a microgrid to formulate the background for the microgrid design.

Solar photovoltaic (PV) systems and energy storage (battery) are desirable components for a microgrid. A hybrid microgrid utilizes both AC and DC sources where the energy resources and loads may be split into two groups, AC and DC, and are connected by a bidirectional converter. Inverters are used to convert solar or battery DC power to AC to serve AC loads. Charge controllers enable the PV panels to charge the battery, as well as to prevent the power running from the battery to the solar panels [4-7].

Normally, a microgrid operates in synchronization with a large grid and this operation is termed as grid-connected mode. However, in the absence of the large grid, the distributed generators in the microgrid must be controlled to maintain its rated voltage and frequency. In this stand-alone or autonomous mode, the microgrid supplies its own load [8-10].

When the microgrid is in stand-alone mode, the fault current is very low due to low short circuit capability. This leads to many protection issues such as relay miscoordination, sympathetic tripping, fuse-recloser miscoordination, delayed operation or blinding of protective relays. The proper relay system operation will prevent any damage to the microgrid [11-13].

Energy router is one of the core equipment for a microgrid community. To coordinate the power flow among its terminals, a centralized control is typically applied. Centralized control relies on communications with a central controller and has lower reliability and flexibility. A novel control strategy has been investigated to achieve distributed power flow control without central controllers [14].

Load management in a microgrid is critical. Load management should be efficient and reliable where appropriate prioritization of loads is important. Examples of top-prioritized loads are hospitals and police stations [15].

The load management and balancing in a microgrid is also handled based on data from sensors at its circuit breakers. If the sensed data show more loading for a circuit than its pre-determined threshold, a neighboring circuit may be used to handle part of the load so as to mitigate the overloaded circuit. Load balancing is performed to ensure no single overload happened on the line and this should be done in real time. Energy storage plays an important role in balancing generation and power demand in a microgrid. It can store surplus generated power while releasing the stored power when needed to supply the microgrid load [16-18].

Our microgrid design considers the aforementioned features regarding functionality and operation of a microgrid. A goal for the design is to obtain a microgrid that can supply power adequately to a community without any dependence on the large grid. Another goal is to make the microgrid smart in the sense that it can control its operation automatically.

2. Theoretical design of realistic stand-alone microgrid

Our design aims to power a small community that includes essential buildings such as residential homes, schools, a hospital, stores, and so forth. The goal is to supply power by mainly relying on solar panels and batteries. To support the peak power of the community and for emergencies we incorporate a diesel generator. This way, the microgrid is self-sustained to provide power to the community.

2.1 Creating load model and circuit design based on real-world data

We use the community in downtown of El Monte city, California, to develop the microgrid load model and distribution circuit layout. The downtown area is shown in Fig. 1 where its boundary is marked by yellow line.

Southern California Edison (the utility power company for the chosen area) online portal provides the total power consumption of the area. The online portal provides the grid lines that power the area of El Monte with data of each respective grid line. As seen in Fig. 2, there are three grid lines in the area, which are Columbia, Daroca, and Enloe. These gridlines give the total power consumption of the area load which is 18869 kWh per day. This area has 176 residential

buildings and 37 commercial buildings that include El Monte courthouse, a school, medical clinic centers, churches, stores, senior apartments, and a bank.

Power consumption estimation for chosen area

The residential and commercial power consumption of our chosen area is estimated using residential energy consumption surveys from the U.S. Energy Information Administration (EIA) and energy data reports from Southern California Edison [19, 20]. Such data yields annual energy consumption of our chosen area. Dividing the annual energy consumption by 12 months yields the average energy per month, while dividing the annual energy consumption by 365 days yields average energy consumed per day. The average real power per day is calculated using the average energy per day and dividing by 24 hours. The power consumption findings are provided in Table 1.

Microgrid circuit design

After finding all power consumptions, a distribution circuit layout is developed for the community (Fig. 3) The microgrid consists of 3-phase and single-phase loads connected to three feeders. The summation of power and energy consumed by all loads in Fig. 3 matches the load data in Table 1. The loads are supplied by a solar system and a battery bank through an inverter, and a diesel generator. A capacitor bank is used to supply reactive power.

After the generated electricity is converted from DC to AC through the inverter, the 22kV AC output is distributed through a 3-phase 4-wire system to different loads of the community. The distributed lines are connected to smaller transformers, which reduce the voltage from 22kV to 120/240V for residential houses. The 22-kV voltage is reduced to 240V or higher for commercial buildings. Residential houses use single-phase power while high-demand commercial buildings (auto shop, church, hospital etc.) use 3-phase power distributed through 3-phase transformers. These transformers are located either outdoors or inside buildings as permitted by code [21, 22]. The conductor used for the power lines is 556,500 26/7 ACSR and the conductor for the neutral is 4/0 ACSR.

Table 1 Average energy and power consumption for load model based on El Monte city, California

Parameter	Value
Annual Energy (kWh)	6,887,500.00
Average Energy Per Month (kWh)	573,958.33
Average Energy Per Day (kWh)	18,869.86
Average Real Power Per Day (kW)	786.24

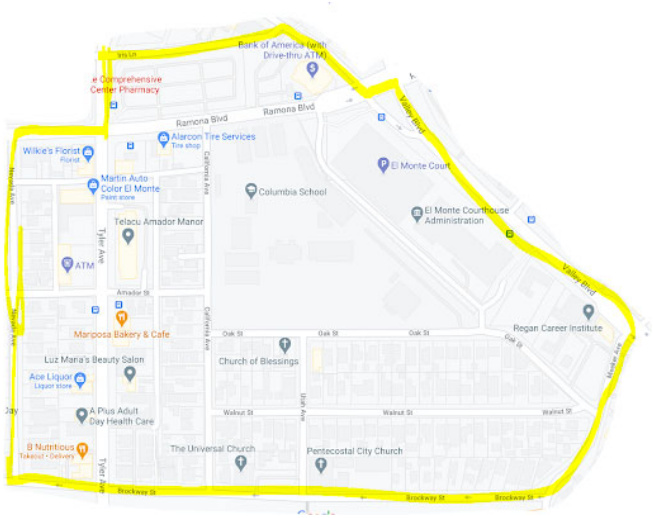

Fig. 1 Air view of the chosen area in El Monte city, California. The yellow line marks the area boundary.

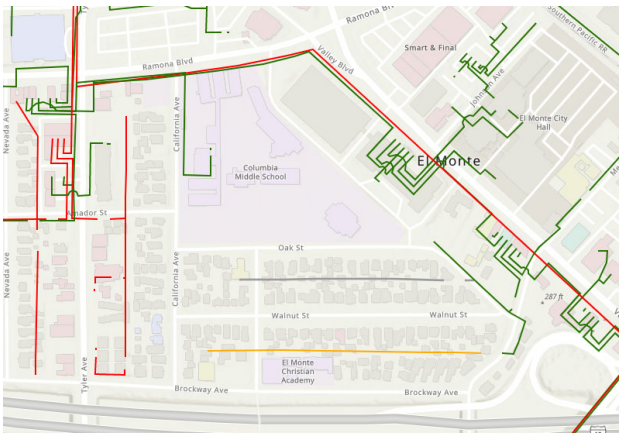

Fig. 2 Air view of chosen area in El Monte city, California, showing the different grid lines in the area. The red line is the gridline of Columbia, the green line is of Enloe, the yellow line is of Daroca. The gray line is also Daroca but is a single-phase line.

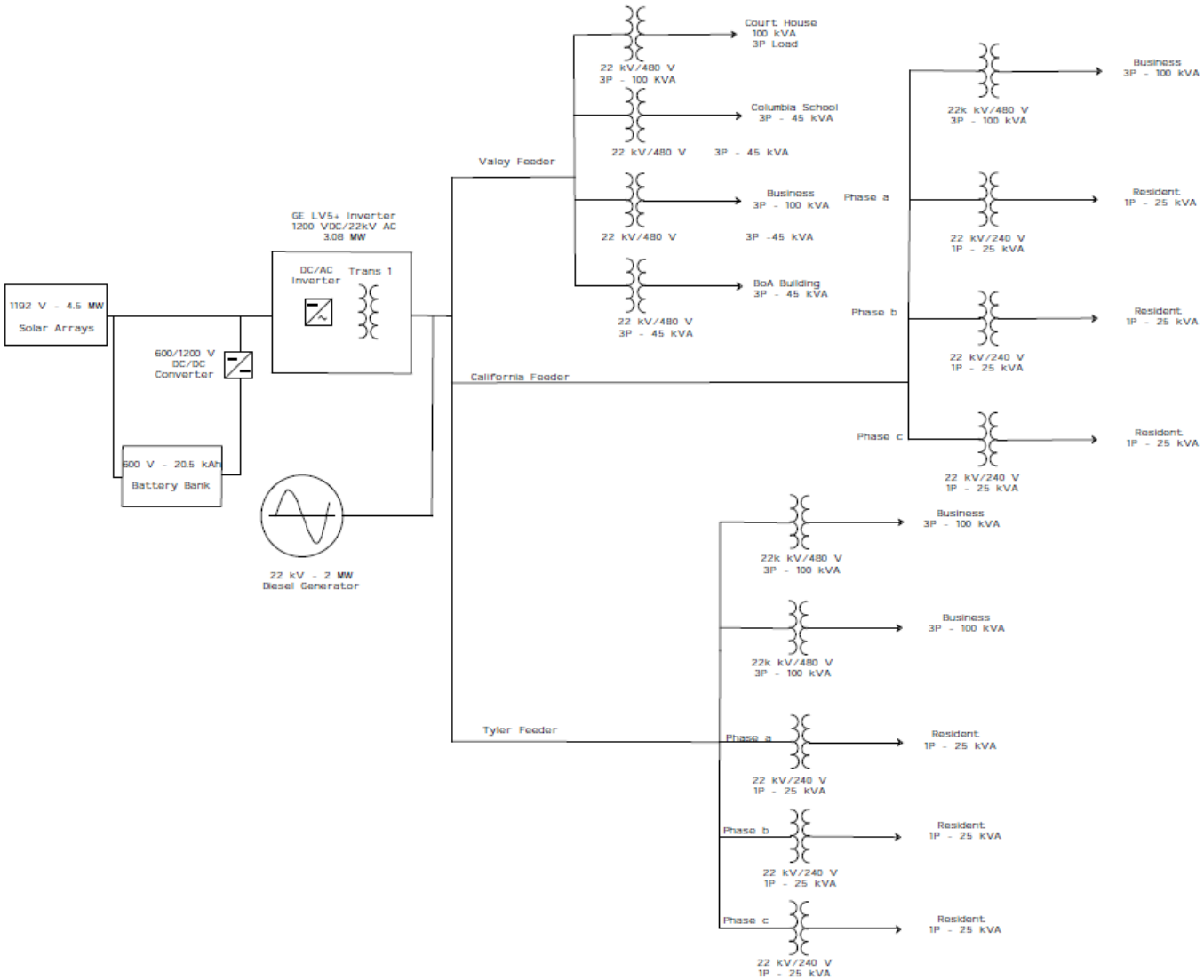

Fig. 3 AutoCAD distribution circuit layout for the microgrid

Peak power and reactive power demand

The U.S. Energy Information Administration (EIA) provides the demand of energy in different regions within the U.S. for every hour [23]. Given that El Monte is located close to the district of Los Angeles, data from 2019 of Los Angeles Department of Water and Power (LADWP) can be used for El Monte. The data from Los Angeles help model El Monte's load so that El Monte's load can be displayed for every hour for a whole year. This yields the times of day and month where we have peaks and lows. Table 2 shows the derived peak load demand for the load model based on El Monte city for 12 months. The highest monthly power demand is 1837.9 kW (peak demand in June). The average power consumption per month is 786.24 kW. Detailed calculation is given in the Appendix.

All residential loads (single-family houses) in Fig. 3 are assumed to have a peak real power demand of 4 kW, based on commonly known typical power demand for U.S. single-family houses. A power factor of 0.9 lagging is used for the microgrid total load. Equations (1), (2), (3), and the peak demand in June (Table 2) are used to calculate the microgrid apparent

Table 2 Peak power of load model based on El Monte city for 12 months

Month	Jan	Feb	March	April	May	June
Peak Power (kW)	1425.3	1403.0	1413.9	1467.1	1490.7	1837.9
Month	**July**	**Aug**	**Sep**	**Oct**	**Nov**	**Dec**
Peak Power (kW)	1736.0	1607.5	1757.5	1634.0	1495.9	1388.0

power, reactive power demand and the rating of the capacitor bank used to supply the reactive power [24].

$$S = \frac{P}{Power\ Factor} = \frac{1837.9}{0.9} = 2042.1(KVA) \quad (1)$$

where S is the apparent power, P is the peak power.

$$Q = \sqrt{S^2 - P^2} = \sqrt{2042.1^2 - 1837.9^2} = 890\ (KVAR) \quad (2)$$

where Q is the reactive power.

$$C = \frac{Q_C}{\omega V_{RMS}^2} = \frac{890kVAR}{2 \cdot pi \cdot 60 \cdot 22kV^2} = 4.877\ (\mu F) \quad (3)$$

where C is the capacitance of the capacitor bank to be used in the microgrid to supply its reactive power demand in a worst-case scenario where the system peak real power demand is 1837.9 kW.

Load allocation and number of needed single-phase transformers

Referring to Fig 3, the microgrid load is allocated so that the system loading is balanced. Every commercial facility is supplied by its own 3-phase step-down transformer from a 3-phase power line. For allocating single-phase loads (single-family houses) we divide the residential houses into groups to determine the number of needed transformers. The total number of the residential houses is 176 while a single-phase transformer can serve 8 houses. It follows that 22 single-phase transformers are needed. The method we use to determine the number of transformers is based on [17, 22, 25]. Out final design has 21 single-phase transformers where 18 transformers supply 144 houses (each supplies 8 houses), 2 transformers serve 22 houses (each serves 11 houses) and 1 transformer serves 10 houses. This load allocation method helps minimize the system load imbalance.

Note that not all single-phase transformers are shown in Fig. 3 to make the figure clear.

2.2 Solar PV system size and energy production

The solar PV system is designed to supply all the energy demand of the microgrid. The daily average energy consumed by the load is used to find the size of the solar system. Because there are losses in the distribution lines and inverter, we increase the daily average energy consumed by 10% to account for the losses. The model chosen is the Trina 400W Solar Panels 144 ½ Cell Multi-BB Mono TSM-400-DE15H(II). Table 3 shows its main characteristics. The energy produced by the solar system is calculated using an equivalent 5.5 peak-sun hours per day for El Monte area [26, 27] and the results are shown in Table 4.

The average energy demand that accounts for losses is divided by the peak-sun hours which converts the output needed into watts. We multiply this value by the efficiency of the solar panels (19.7%, Table 3) to obtain the size for the solar system [28]. This yields a DC solar system size of 4517.45 kW, as shown in (4).

Table 3 Solar panel characteristics

PV panel characteristics	
Max Power Point Voltage (Vmpp) – (V)	47.40
Max Power Point Current (Impp) – (A)	9.74
Maximum Power Point (Pmax) – (kW)	0.46
Efficiency (%)	19.70

Table 4 Power and energy production of solar system

Parameter	Value
Annual Energy Production (kWh)	39,572,862.00
Average Energy Production per Month (kWh)	3,252,564.00
Average Energy Production Per Day (kWh)	108,418.80
Average Power Production (kW)	4517.45

$$DC\ Solar\ System\ Size = \frac{Daily\ kWh \times 1.10}{Avgerage\ Sun\ Hours} \times efficiency\ factor$$
$$= \left(\frac{20756.85\ kWh}{5.5\ hours}\right) \times 1.197 \quad (4)$$
$$= 4517.45\ kW$$

The city of El Monte is located in the northern hemisphere. Therefore, the fixed solar panels should face south and they should be tilted at an angle of 34.07 degrees (latitude of the city) to maximize the annual energy gain [24, 29, 30].

Our solar system size is double-checked using PVWatts Calculator of the U.S. National Renewable Energy Lab (NREL) [31]. On the NREL website, one can enter the location of the solar system, tilt angle, and its size. The PVWatts Calculator will output how much energy this system will produce in a year. The outcome matches our calculations shown in Table 4.

The chosen solar system ratings of 1192V and 4517kW require 8175 panels. They would occupy 4.17 acres of space. The cost of the solar system is estimated to be $1,753,758 U.S. dollars. Figure 4 shows the chosen location for the solar panel arrays.

2.3 Battery and inverter rating

The demand of the microgrid load is the main factor considered for choosing the battery system. Other considered factors are the battery cost (capacity per cost-of-unit), size (dimensions), and safety. This leads us to choose lithium-ion Samsung 30Q-18650. The Samsung battery offers good capacity per cost-of-unit as compared to other batteries. Furthermore, it is easy to configure the battery cells thanks to their cylindrical shape. It is covered in metal which makes it less prone to catch fire compared to lithium-polymer cells and pouch cells.

The rating of a battery cell or nominal energy is 10.8 Wh. The battery system is used before sunrise and after sunset to supply the microgrid load. The shortest day in Southern California is 9 hours and 55 minutes which means that we need the battery system to provide power for up to 14 hours and 5 minutes per day [32].

Given the demand of our system, the energy required from the battery is 11,443.15 kWh. Multiple battery cells are connected in series and parallel to obtain the

Fig. 4 Air view image using Google Maps showing the three chosen locations for the solar arrays. The arrays are placed near inverter, battery, and diesel generator to reduce power losses due to wiring.

Table 5 Battery cell characteristics

Samsung 30Q-18650 cell characteristics	
Max discharge current	20A
Max continues discharge current	15A
Nominal voltage (V_{bat})	3.6V
Cutoff voltage	2.7V
Capacity (at 10A discharge)	3 Ah
Nominal energy $C_{ideal} = (3.6V * 3Ah)$	$10.8\ Wh$
Capacity of a cell with 70% and Depth of Discharge (DOD) $C_{DOD} = 10.8Wh * 0.7$	$7.56\ Wh$
Capacity of a cell with 95% Discharge Health (C) $C = 7.56Wh * 0.95$	$7Wh$

Table 6 Inverter characteristics

Inverter LV+ 1560 Solar Power Station (853-1300)	
Maximum Permissible DC Voltage (Vdc)	1500 V
Maximum Continuous DC Current (at 35°C / 50°C)	4000/3200 A
Active AC Output Power (PF = 1)	3.08/2.73 MW
AC Output Voltage (+10% / -10%)	22/33/34.5 kV AC
Maximum AC Current (at 50°C)	72/48/46 A AC
Maximum AC Current (at 35°C)	82/55/52 A AC
Grid Frequency ±5%	50/60 Hz

required power capacity. The chosen battery ratings are 600VDC, 20,500 Ah or 13.296 MWh. The battery estimated cost is 7,750,122 U.S. dollars.

The rating of the inverter used to convert the DC power generated from the PV system and the battery into AC is chosen based on the battery and solar system size. The calculated inverter power loss of 1769.05 kWh (i.e. about 15%) is included in its sizing. The chosen ratings for the inverter are 1200V DC/22kV AC 3.08MW.

The characteristics of the battery cell and the inverter are provided in tables 5 and 6. The battery configuration and calculation are provided in the Appendix.

2.4 Diesel generator rating

The diesel generator is used to support the microgrid peak load conditions during any day and under unfavorable conditions, such as cloudy days or other emergency situations. Recall that the system peak power demand of 1837.9 kW happens in June (Table 2). It is estimated that the generator should produce up to 2000kW.

The model chosen for the diesel generator is the CAT 3516C 2000kW 480VAC Diesel Generator [33]. According to [34], there are 282 sunny days and 83 cloudy days per year in El Monte. On sunny days, the diesel generator is used for around 3 hours to support the peak load at 92-percent of its rating. On cloudy days, the generator is used for around 13 hours per day at 50-percent of its rating. The generator estimated price is 435,000 U.S. dollars. The total cost of fuel to operate the generator is 738,423 U.S. dollars per year. Detailed estimated costs and expenses related to the diesel generator are given in the Appendix.

2.5 Control system

The control system manages the microgrid generators, battery and loads. It determines suitable energy allocation schemes based on the system demands. Energy from the battery can be drawn to prevent shedding load while excess generation must be absorbed by either reducing generation, increasing load, or charging energy storage [15]. To preserve the battery life, the depth of discharge is limited to 20%. The control system flowchart is shown in Fig. 5.

Pseudo code for control logic of Fig. 5

START. Sensors read voltage and amperage through all circuit breakers from PV and BAT.

IF the PV power produced is more than load demand, the surplus power is used to charge the battery until it is fully charged. Once it is fully charged, the battery will be isolated.

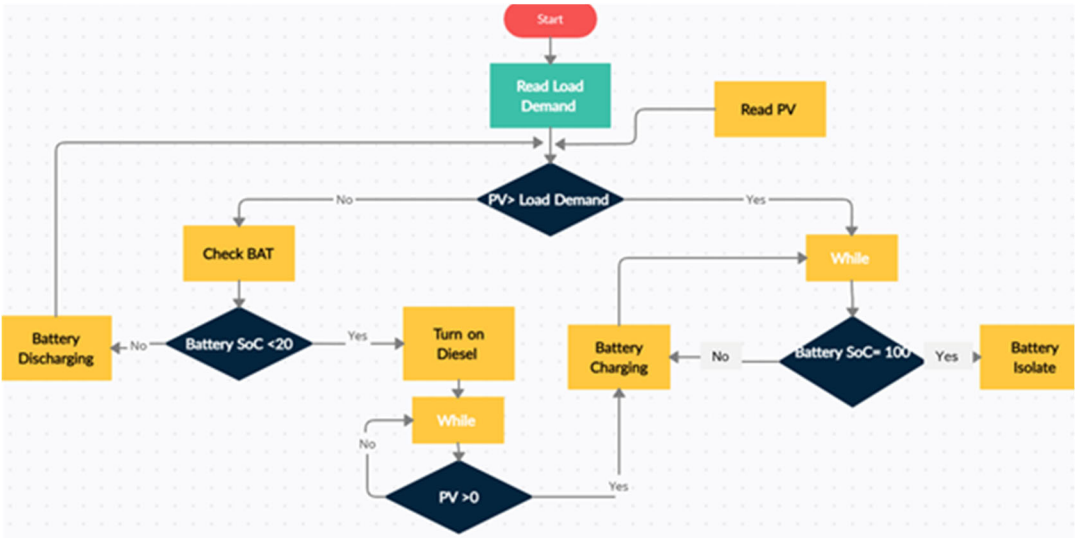

Fig. 5 Flowchart of microgrid control logic

IF the PV power produced is less than load demand and if the battery state of charge (SOC) is equal or greater than 20%, the battery system will begin discharging to supply energy needed by the load demand.

IF the PV power produced is less than load demand and if Battery SOC is less than 20%, the Diesel Generator (DG) will be on to supply load demand. While the DG is on, PV power, if any, will be used to charge Battery.

START. Continuously read and compare the battery state of charge, PV power, and load demand.

3. Implementation of microgrid design for simulation

Our microgrid design is implemented and simulated using MATLAB Simulink Specialized Power Systems and Stateflow toolboxes. Figure 6 shows an overview of our microgrid implementation. The main subsystem blocks include solar PV system, battery system, converter/inverter substation, diesel generator, control system, and distribution system. These main subsystems are composed of blocks and/or subsystem blocks. The parameters of main blocks are provided in the Appendix.

3.1 Solar system implementation and testing

We input parameters from the solar panel data sheet to Simulink Solar Panel block. The annual average solar radiation of 6.21kWh/m^2/day for El Monte city is found using the website PVWATTS.nrel.gov [31].

Dividing the found radiation by a value of 8 sun hours per day yields an irradiance value of 776 W/m^2. Hence, we use input irradiance values of 200, 600, 1000 W/m^2 for testing of the solar system. These values model the varying irradiance throughout a normal sunny day depending on the sun position.

The Simulink Solar Panel block produces DC output voltage which is used to charge the battery directly or be boosted to 2400VDC to supply the load through the inverter.

Figure 7 shows the Simulink-based solar PV system while Fig. 8 shows its power and voltage for three different irradiance values. It produces 3.7 MW and 1200V at an irradiance of 1000W/m^2, 2.2 MW and 1250V at 600 W/m^2, and 0.55 MW and 1150V at 200 W/m^2. The results show that the solar system operates normally.

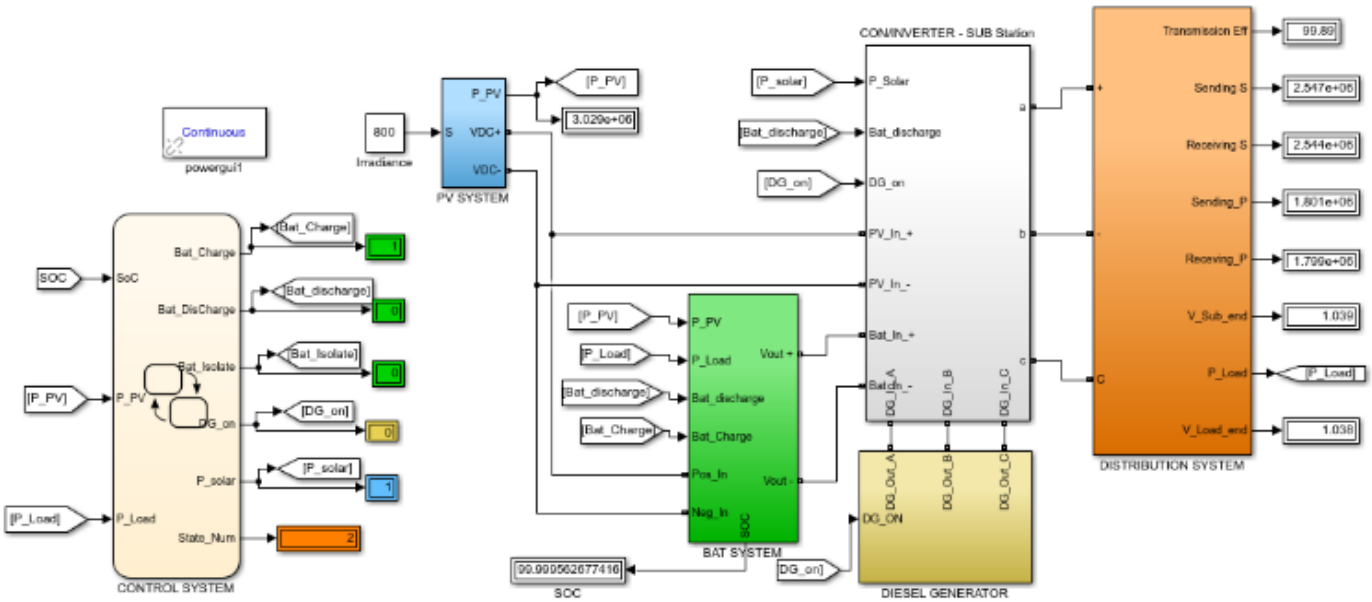

Fig. 6 Microgrid design implemented using MATLAB Simulink

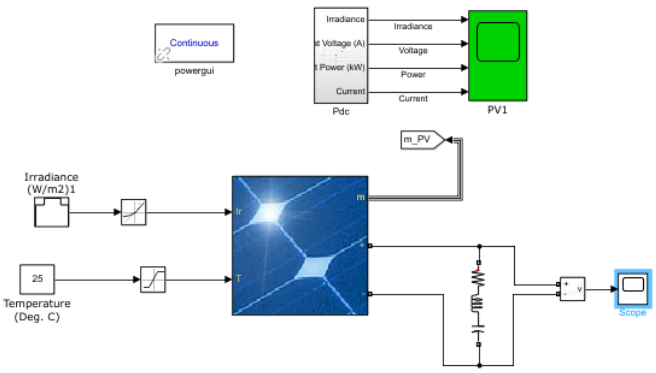

Fig. 7 Simulink-based PV system. Solar Panel Block receives varying input of irradiance. Temperature is 25^0C which is a standard test condition.

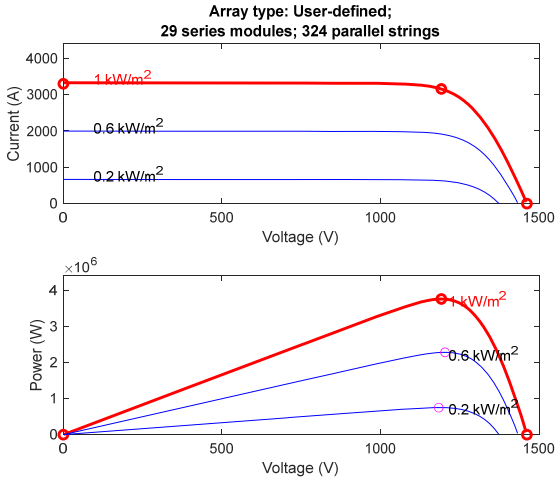

Fig. 8 Current, power, and voltage generated by PV system for three different irradiance values

3.2 Battery system implementation and testing

The battery ratings of 600 VDC, 20,500Ah and13.296 MWh are the inputs for Simulink Battery block. Figure 9 shows the battery subsystem implementation while its block parameters are provided in Appendix.

The battery system is tested at different discharge power conditions. At nominal discharge power of 786kW (1310A), the battery system can supply the microgrid average load (786kW, Table 1) for 15.5 hours. At maximum discharge power of 1.8378 MW (3063A), it can supply the peak load for 5.5 hours. Plots of its discharge characteristics are shown in Fig. 10.

3.3 Diesel generator testing

The diesel generator (DG) is obtained by modifying a synchronous machine block from a Simulink unpublished project designed by Dr. Ha Le [24, 29, 30].

Based on the data sheet of the DG, the parameters of the block are 2500kVA, 480VAC at a frequency of 60Hz. Since the DG output voltage is 480VAC while the output voltage of the inverter is 1100VAC, the DG output is connected to a step-up transformer to increase its voltage to 1100VAC for connection with the inverter. Figure 11 shows the Simulink-based DG system.

3.4 Distribution system implementation

The Simulink-based distribution system is shown in Fig. 12 where the microgrid load is modeled using four blocks. By combining the loads, we limit the number of components which allows simulation to run faster.

One block represents the 3-phase load of commercial buildings. The load is 3-phase Y-ground with a nominal voltage of 480V. The residential homes are connected to the 3-phase line where Phase A and Phase B supply 59 homes each while phase C provides power to 58 homes. All the 176 homes are served at a nominal voltage of 240V through single-phase transformers.

3.5 Inverter, boost converter, and LC filter

The boost converter and the 3-phase inverter are built by referencing the Power Electronic textbook by Daniel Hart [35]. The 3-phase inverter is designed to convert the DC voltage of the solar system and the battery to AC voltage. The boost converter is used to raise the voltage output of the solar system to a level that is beneficial to the inverter. Ideally, to keep the voltage output of the inverter constant, its voltage input must be higher than its expected ideal rating.

The pulse width modulation (PWM) technique used for the inverter is obtained from [36]. Additionally, an LC filter is used after the 3-phase inverter to remove the unwanted harmonics that distorted its output waveform. The Simulink block diagrams of the inverter, the boost converter and the LC filter are provided in Appendix.

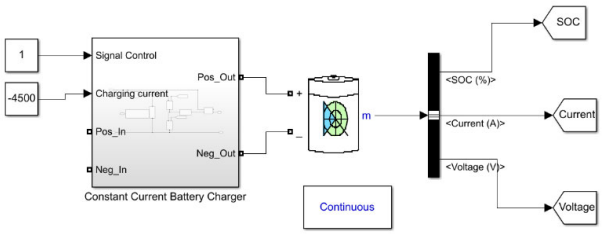

Fig. 9 Simulink-based battery system

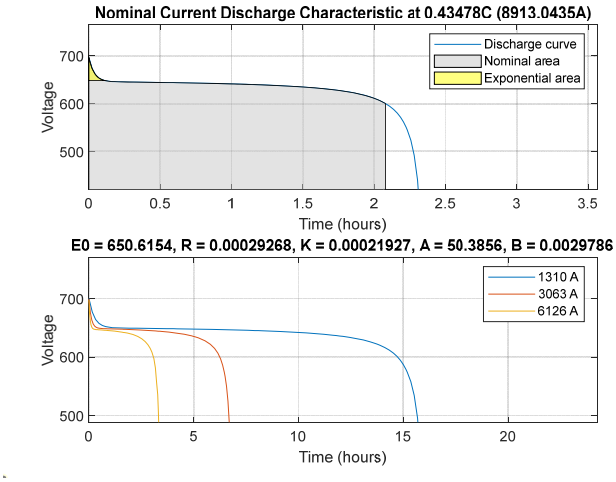

Fig. 10 Discharging characteristics of battery system

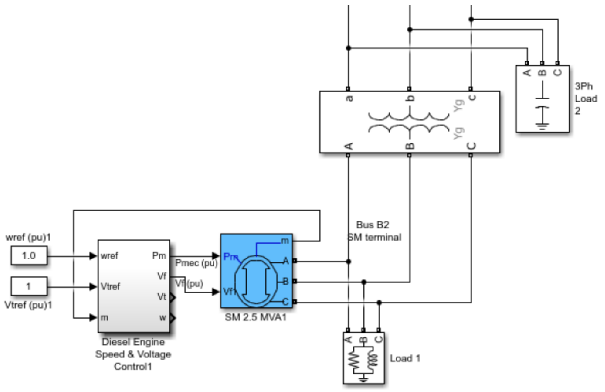

Fig. 11 Simulink-based diesel generator system

Fig. 12 Simulink-based distribution system

3.6 Control system implementation and testing

Simulink Stateflow is a graphical environment that allows one to design and simulate decision logic for supervisory control, task scheduling, and fault management applications [37]. A state flow can be one set of states where the state machine can be in one state at any given time. The current state depends on the previous state and the transition between states is executed based on conditions and variables. A state transition can be executed unconditionally [38].

For our control system described in Section 2.5, we represent five states using a finite state machine. The Simulink-based state flow for the control system is shown in Fig. 13.

The operational principle for the controller state flow is as follows. A state can have an Entry and an Exit action. A state configured as a final state may have only an entry action. When a workflow instance enters a state, any activities in the entry action are executed. When the entry action is complete, the triggers for the state's transitions are scheduled.

When a transition to another state is confirmed, the activities in the exit action are executed, even if the state transitions back to the same state. After the exit action completes, the activities in the transition's action execute. Then, the new state transition takes place, and its entry actions are scheduled [39]. For example, the initial state is set by using entry actions such as Battery isolate, no PV power, and Diesel Generator turn off. To move from State 1 to State 2, we need the condition where the battery state of charge is less than 100% and PV power is greater than Load Demand.

When a state machine starts, an entry defines which state will be activated first. An exit is used to deactivate a state. For example, in entry state 3, Battery Isolate is set to 1 and exit Battery Isolate set to 0. This means that when leaving state 3, the battery is no longer isolated, and it will be charged or discharged in other states.

State Flow charts receive inputs of PV Load, Battery's State of Charge, and Load Demand from Simulink and provide outputs (commands) to control systems through switches. Testing shows that the controller state flow transitions from one state to another accurately.

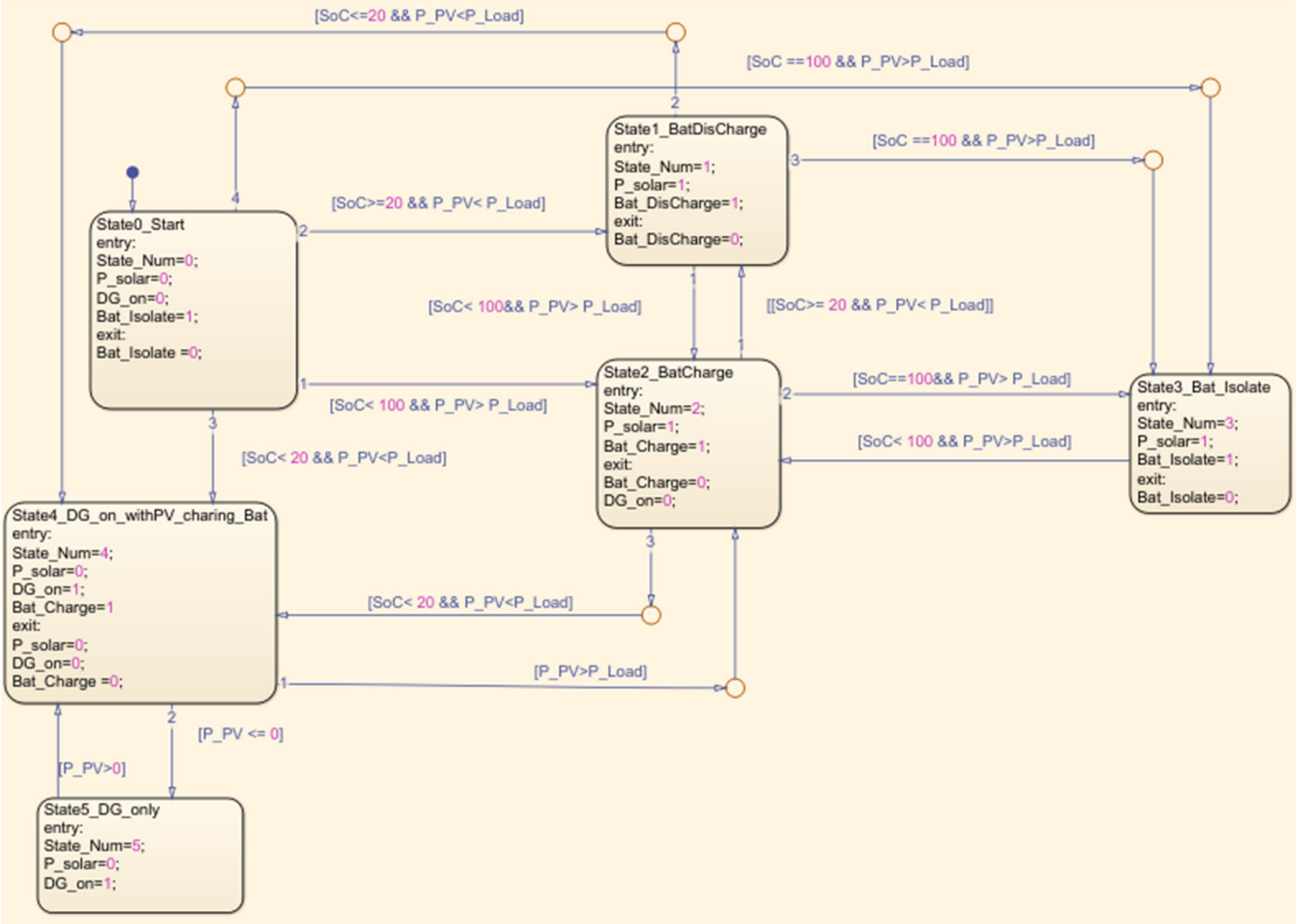

Fig. 13 Simulink-based state flow for microgrid control system

4. Simulation results

For evaluating the microgrid operation, we simulated five scenarios. Each scenario or state corresponds to a scenario that we expect to happen in real-world environment.

1) State 1: Battery supplies load demand only, no PV or DG is used

In this scenario, we simulated to meet the demand of the peak load using the battery alone. The solar PV system and DG are turned off.

Assuming an SOC of 100% for the battery, the maximum output of the battery is 12MW which successfully supplies the load demand of 1.8MW. As the battery discharges, the maximum output of the battery will decrease but our battery is designed to supply the peak load for 15 hours. We expect this scenario to happen mainly at night when there is no sunlight available for the solar system.

2) State 2: Solar PV system supplies load and battery is being charged

In this scenario, we simulated to meet the demand of the load using only the power generated by the solar PV system, assuming an irradiance of 1000W/m^2. We expect this situation to occur in the middle of the day where the sunlight is at its brightest and the solar system can successfully supply load and charge the battery at the same time.

In this scenario, the PV system is delivering power, the battery is being charged, and the diesel generator is turned off. Simulation results show that the output of the PV system is 3.7MW, which is more than enough to supply the power demand of 1.8MW. The surplus power is used to charge the battery.

3) State 3: Solar PV system supplies load and battery is fully charged

This scenario can occur at around 4pm during summer when irradiance is still high at about 600W/m^2. At this time, the battery becomes fully charged and it is isolated (disconnected) from the system. The solar system keeps supplying the load, while the DG remains off.

Simulation with an irradiance of 600 W/m^2 and battery SOC of 100% shows that the voltage of the load is 0.995 per unit. The solar system produces 2.1MW which exceeds the maximum load demand of 1.9 MW.

4) State 4: Diesel generator supplies load, load demand exceeds solar system power output and battery is charging

This scenario can happen in the early morning hours or during winter time when the irradiance is low so the solar system does not produce enough power for the microgrid. The battery SOC is less than 20%. We ran the simulation with an irradiance of 200W/m^2 and battery SOC of 19%. The control systems activates the diesel generator to supply the load which yields a load voltage of 1.006 per unit. The solar system produces 0.323 MW which is used to charge the battery.

5) State 5: Diesel generator supplies load

In this scenario, there is no power generated by the solar system and the battery's SOC is lower than 20% after 15 hours of discharging. Since there is not enough power from the solar system or the battery, the microgrid relies on the diesel generator to supply the demand. We expect this situation to happen in very cloudy days, rainy days, nighttime, or emergency conditions where there is little or no solar power.

In this simulation state, the diesel generator is on while the solar system and the battery are both off. Simulation results show that the diesel generator can supply the load demand of 1.9 MW where the load voltage is 0.9868 per unit, and the power distribution efficiency is 99.89%.

5. Conclusion

In this project a microgrid is developed based on downtown community of El Monte city, California. The system main components include a solar PV system, a battery, a diesel generator, an inverter, a control system, and loads. The microgrid design is simulated using MATLAB Simulink and the results have led to the following conclusions:

1) The microgrid can supply power to its community adequately and independently without relying on any utility power grid.
2) The microgrid is smart as it can operate autonomously thanks to its automatic control system.
3) Under different operational scenarios, the microgrid proves to be resilient where it can supply its load demand using various sources (solar system, battery, diesel generator). The load voltage is maintained at satisfactory values of around 1.0 per unit. The power distribution efficiency is at least 99% showing the system low losses.

For future work, we would like to perform an economical analysis to evaluate the cost effectiveness of the power supply in the microgrid. We also plan to improve the control system and the generation-load balancing scheme.

The microgrid design is expected to contribute understanding and experience to develop similar systems for use around the world. The use of the smart microgrids will help improve the reliability and resiliency of large power grids, as well as provide energy independence to communities.

Appendix

A. Calculation of peak load

Eia.gov gives the data of the demand energy for each month, each day, and every hour [23]. Knowing that the Daily Average Energy (DAE) is 18869.86kWh and the Daily Real Average Power is 786.24 kW, the data of eia.gov is scaled down to match our DAE. For example, in Los Angeles during January, the total demand energy is 71486.41935MWh, and on 1/1/2019 at 12a.m., the demand energy is 2804MWh. To find the peak power on that date and hour, the following ratio in (5) is used:

$$P(peak) = \frac{2804\ MWh}{71486.41935\ MWh} * 18869.86\ KWh/1h = 740.16\ \text{KW} \quad (5)$$

The same method above is repeated for each hour in every month. Having the power for each hour yields the peak power of each day and month. The maximum peak power is found to be during June with a consumption 1837.9kW.

B. Battery related calculation

Battery calculations are based on average energy demand for a single day (*Edaily*):

$$E_{daily} = 18869.86\ kWh$$

Battery system is used before sunrise and after sunset. The shortest day in Southern California has 9 hours and 55 minutes which means that we need the battery system to provide at least 14 hour and 5 minutes [32]. We use 15 hours for our calculation with 10% extra for fluctuation.

The energy that the battery system needs to provide during nighttime (E_1):

$$E_1 = 18{,}869.86\ kWh * \frac{15hrs}{24hrs} = 11{,}793.66\ kWh \quad (6)$$

Loss by inverter ($E_{Inverter_{Loss}}$) (DC to AC inverter cause 15% power/energy loss):

$$E_{Inverter_{Loss}} = E_1 * 0.15 = 1769.05\ kWh \quad (7)$$

Energy needed include loss by inverter (E_2):

$$E_2 = E_1 + E_{Inverter_{Loss}} = 13{,}562.71\ kWh \quad (8)$$

Number of cells needed based on the energy demand and cell capacity

$$\#Cell = \frac{E_2}{C} = 1{,}937{,}530\ cells \quad (9)$$

System Voltage: We chose system voltage (V_{sys}) to be 1185V (25 panels in series x 47.4V per panel=1185V) since the maximum system voltage of the solar panel is 1500V.

Number of cells in Series.

$$\#Cells_{Series} = \frac{V_{sys}}{V_{bat}} = 320\ cells \quad (10)$$

Number of cells in parallel

$$\#Cell_{Parallel} = \frac{\#Cell}{\#Cell_{Series}} = 5886\ Cells \quad (11)$$

System continuous current (I_{sys})

$$I_{sys} = \#Cell_{Parallel} * I_{cell} = 1.24\ kA \quad (12)$$

System continuous power (to the battery last 15 hour, the battery needs to discharge at 0.21A/h)

$$P_{sys} = V_{sys} * I_{sys} = 11{,}443.00\ kW \quad (13)$$

Maximum current that the battery can supply (Battery discharge at 10A rate)

$$I_{max} = \#Cells_{parallel} * 10A = 58.86\ kA \quad (14)$$

Maximum power that the battery can supply (at 10A discharge rate)

$$P_{max} = V_{sys} * I_{max} = 69.75\ MW \quad (15)$$

Cost of battery

$$Cost = \#Cells * Cost_{Cell} = \$7{,}750{,}122.31 \quad (16)$$

C. Estimated costs and expenses of diesel generator

The estimated costs and expenses of the diesel generator are shown in Table 7.

Table 7 Costs and expenses of diesel generator

2000 ekW : CAT 3516C - EPA Tier 2					
	Power load (kW)	**Fuel Consumption (gal/h)**	**Fuel cost per hour ($)**	**Fuel cost for 282 Sunny days ($)**	**Fuel cost for 83 Cloudy days ($)**
92% Load	1840	138.9	449.4804	380,260	
75 % Load	1500	107.8	348.8408		86,861
50% Load	1000	77.7	251.4372		271,301
Total fuel cost ($)		738,423		Fuel price/gal ($)	3.236
Generator cost ($)		435,000			

D. MATLAB Simulink block diagrams and parameters

Figures 14-16 show Simulink block diagrams of the inverter, the boost converter and the LC filter.

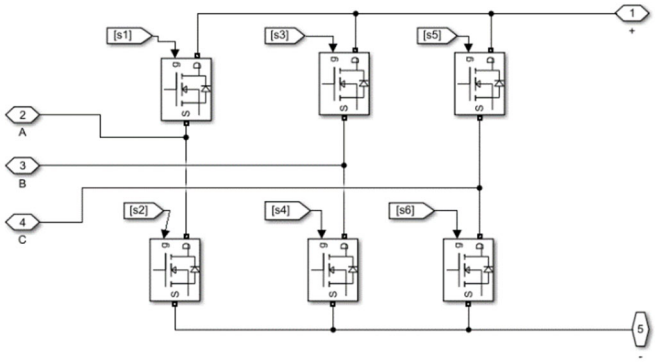

Fig. 14 Simulink-based inverter

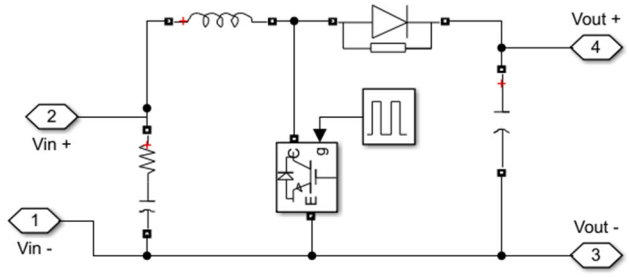

Fig. 15 Simulink-based boost converter

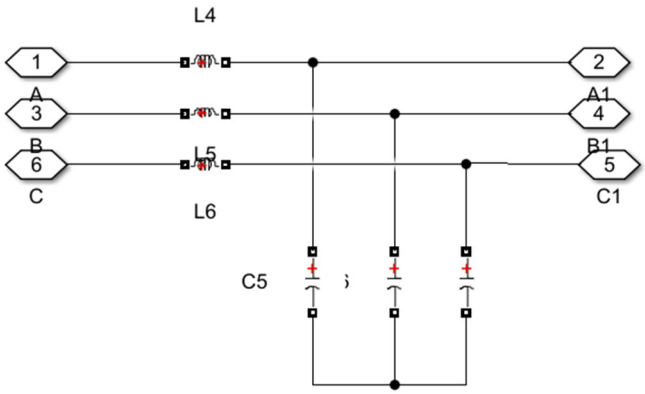

Fig. 16 Simulink-based LC filter

Figures 17-23 show block parameters of main subsystems used in the microgrid simulation.

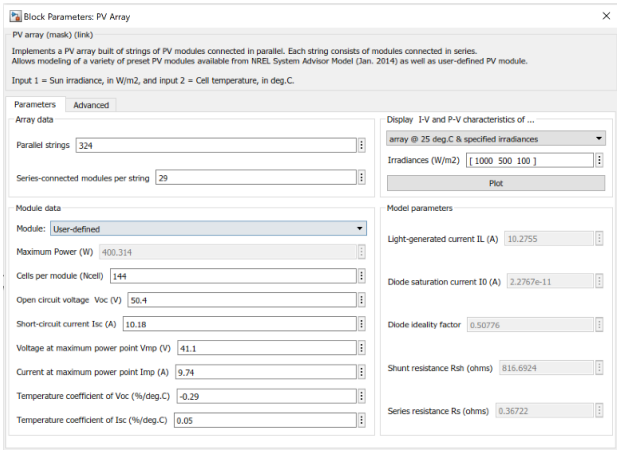

Fig. 17 Block parameters of PV array

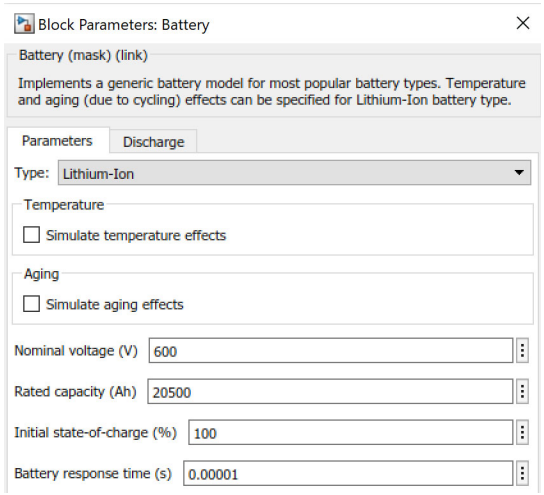

Fig. 18 Block parameters of battery

.

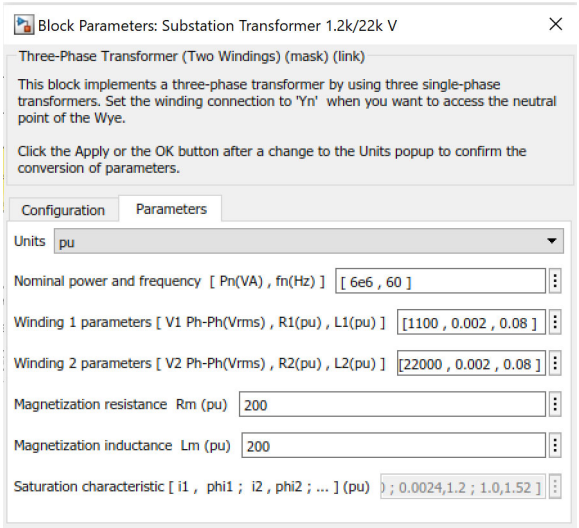

Fig. 19 Block parameters of substation transformer

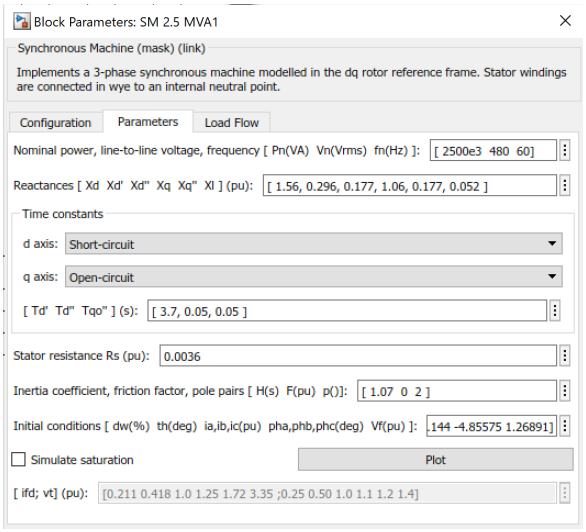

Fig. 20 Block parameters of diesel generator

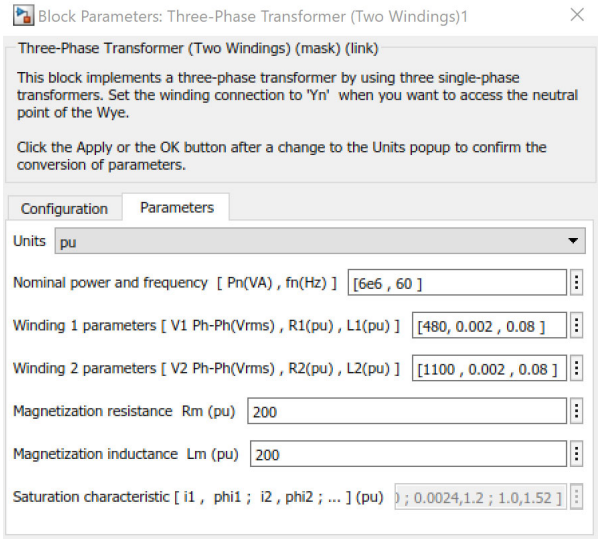

Fig. 21 Block parameters of diesel generator's transformer

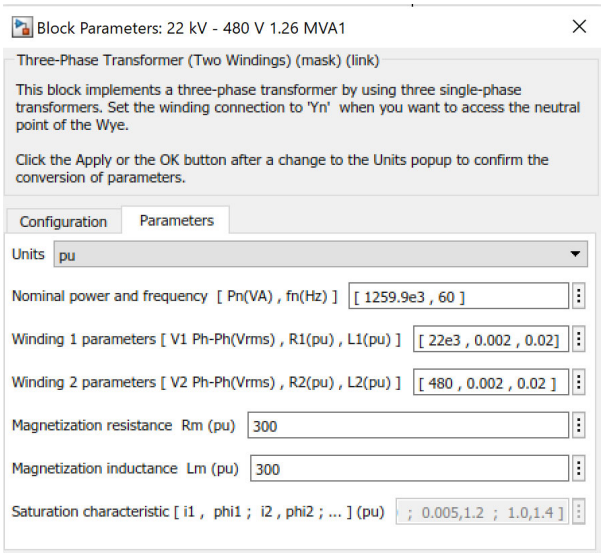

Fig. 22 Block parameters of 3-phase commercial transformer

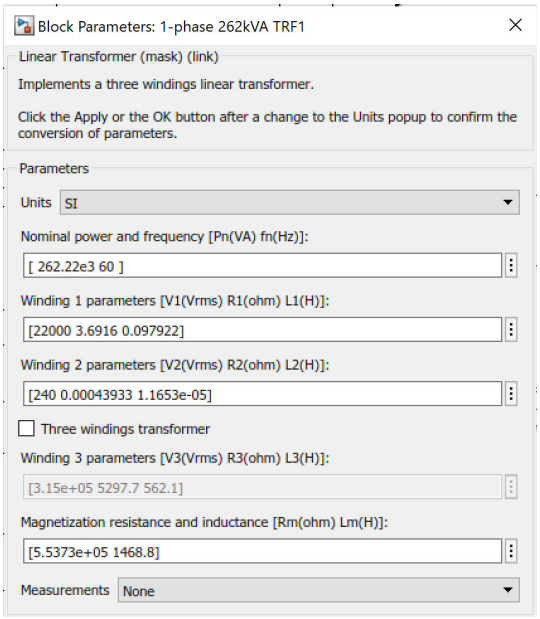

Fig. 23 Block parameters for single-phase residential transformer

Acknowledgement

The student authors gratefully acknowledge and give thanks to Professor Ha Thu Le, our project advisor, for overseeing the project and providing consistent guidance and support throughout the 2020-21 academic year.

References

[1] J. Calderon, J. Cureg, M. Diaz, J. Guzman, C. Rudd, and H. T. Le, "Smart Agriculture: An Off-Grid Renewable Energy System for Farms using Wind Power and Energy Storage," in *Proc. IEEE PES Innovative Smart Grid Technologies Conference*, 2019, pp. 1-5.

[2] B. Postovoit, D. Susoeff, D. Daghbas, J. Holt, and H. T. Le, "A Solar-Based Stand-Alone Family House for Energy Independence and Efficiency," in *Proc. IEEE Conference on Technologies for Sustainability (SusTech)*, 2020, pp. 1-6.

[3] Anh-Huy Le, A. Giourdjian, A. Frankyan, V. Mandany, and H. T. Le, "Design, Sizing and Operation of a Hybrid Renewable Energy System for Farming," in *Proc. IEEE PES Innovative Smart Grid Technologies Conference*, 2016, pp. 1-5.

[4] C. Battistelli, Y. P. Agalgaonkar, and B. C. Pal, "Probabilistic Dispatch of Remote Hybrid Microgrids Including Battery Storage and Load Management," *IEEE Transactions on Smart Grid,* vol. 8, no. 3, pp. 1305-1317, 2017, doi: 10.1109/TSG.2016.2606560.

[5] E. Hossain, E. Kabalcı, R. Bayindir, and R. Perez, "A comprehensive study on microgrid technology," *International Journal of Renewable Energy Research,* vol. 4, pp. 1094-1104, 01/01 2014.

[6] M. Puianu, R. Flangea, N. Arghira, and S. S. Iliescu, "Microgrid simulation for smart city," in *2017 9th IEEE International Conference on Intelligent Data Acquisition and Advanced Computing Systems: Technology and Applications (IDAACS)*, 21-23 Sept. 2017 2017, vol. 2, pp. 607-611, doi: 10.1109/IDAACS.2017.8095164.

[7] Ò. Monés Pederzini, "Design of a Solar Microgrid for the Community of Mpaga, Gabon based on its social and economic context," Universitat Politècnica de Catalunya, 2017.

[8] M. S. Mahmoud, S. Azher Hussain, and M. A. Abido, "Modeling and control of microgrid: An overview," *Journal of the Franklin Institute,* vol. 351, no. 5, pp. 2822-2859, 2014/05/01/ 2014, doi: https://doi.org/10.1016/j.jfranklin.2014.01.016.

[9] Y. Fan, V. Rimali, M. Tang, and C. Nayar, "Design and Implementation of stand-alone smart grid employing renewable energy resources on Pulau Ubin Island of Singapore," in *2012 Asia-Pacific Symposium on Electromagnetic Compatibility*, 21-24 May 2012 2012, pp. 441-444, doi: 10.1109/APEMC.2012.6237907.

[10] M. Barnes *et al.*, "Real-World MicroGrids-An Overview," in *2007 IEEE International Conference on System of Systems Engineering*, 16-18 April 2007 2007, pp. 1-8, doi: 10.1109/SYSOSE.2007.4304255.

[11] V. Vinod and U. J. Shenoy, "An Adaptive Relay Based on Curve Fitting Technique for Micro-grid Protection," in *2020 IEEE International Conference on Power Electronics, Smart Grid and Renewable Energy (PESGRE2020)*, 2-4 Jan. 2020 2020, pp. 1-6, doi: 10.1109/PESGRE45664.2020.9070624.

[12] M. J. Hadidian Moghaddam, M. Bigdeli, and M. Miveh, "A review of the primary-control techniques for the islanded microgrids," vol. 82, pp. 169-175, 08/01 2015.

[13] Y. A. Chau, "Smart grid cooperative communications using switched relays with power allocation," in *2016 IEEE Smart Energy Grid Engineering (SEGE)*, 21-24 Aug. 2016 2016, pp. 376-380, doi: 10.1109/SEGE.2016.7589555.

[14] J. Yu, L. Xiao, Z. Hu, Y. Zhao, and J. Nie, *Multi-Terminal Energy Router and Its Distributed Control Strategy in Micro-grid Community Applications*. 2020, pp. 1028-1033.

[15] B. Moran, "Microgrid load management and control strategies," in *2016 IEEE/PES Transmission and Distribution Conference and Exposition (T&D)*, 3-5 May 2016 2016, pp. 1-4, doi: 10.1109/TDC.2016.7520025.

[16] Z. Cheben *et al.*, "Simulation Board for Smart Service Restoration Schemes in Distribution Grid," *International Journal of Power Systems,* vol. 5, pp. 81-94, 2020.

[17] J. J. Nancy, T. M. S, S. Rohith, S. Saranraj, and T. Vigneswaran, "Load Balancing using Load Sharing Technique in Distribution System," in *2020 6th International Conference on Advanced Computing and Communication Systems (ICACCS)*, 6-7 March 2020 2020, pp. 791-794, doi: 10.1109/ICACCS48705.2020.9074304.

[18] A. Kumar, D. Hussain, and M. Khan, "Microgrids Technology: A Review Paper," *Gyancity Journal of Electronics and Computer Science,* vol. 3, pp. 11-20, 03/31 2018, doi: 10.21058/gjecs.2018.31002.

[19] "Residential Energy Consumption Survey (RECS) - Data - U.S. Energy Information Administration (EIA)." https://www.eia.gov/consumption/residential/data/2015/ (accessed.

[20] "Energy Data - Reports and Compliance." http://origin.sce.com/regulatory/energy-data---reports-and-compliances (accessed.

[21] "120V 240V Electricity explained - Split phase 3 wire electrician." https://www.youtube.com/watch?v=fJeRabV5hNU&ab_channel=TheEngineeringMindset (accessed Dec. 1, 2020, 2020).

[22] R. Baeza. "Selecting, sizing transformers for commercial buildings." https://www.csemag.com/articles/selecting-sizing-transformers-for-commercial-buildings/ (accessed Dec. 1, 2020, 2020).

[23] "United States - U.S. Energy Information Administration (EIA) - Real-time Operating Grid." https://www.eia.gov/beta/electricity/gridmonitor/dashboard/custom/pending (accessed.

[24] H. T. Le, "ECE 3810: Introduction to Power Engineering Lecture Notes," California State Polytechnic University, Pomona, 2019.

[25] "What are the standard single phase and three phase kVA ratings for Transformers by SquareD/Schneider Electric? | Schneider Electric USA." https://www.se.com/us/en/faqs/FA91532/ (accessed Dec. 1, 2020, 2020).

[26] "Solar Energy and Solar Power in El Monte, CA." https://www.solarenergylocal.com/states/california/el-monte/ (accessed 2020/12/17, 2021).

[27] H. T. Le, "ECE 4875: Wind & Solar Power Systems Lecture Notes," California State Polytechnic University, Pomona, 2020.

[28] "How to Size a Solar System: Step-by-Step." https://unboundsolar.com/blog/how-to-size-solar-system (accessed Dec. 1, 2020.

[29] H. T. Le, "MATLAB Simulink: Power system with Synchronous Generator and Asynchronous Motor," California State Polytechnic University, Pomona, 2019.

[30] H. T. Le, "ECE 4875: Simulink Tutorial," California State Polytechnic University, Pomona, 2020.

[31] "PVWatts Calculator." https://pvwatts.nrel.gov/ (accessed.

[32] "Sunshine & Daylight Hours in Los Angeles, California, Usa Sunlight, Cloud & Day length." http://www.los-angeles.climatemps.com/sunlight.php (accessed Dec. 1, 2020.

[33] "WINCO DR500F4 500kW Diesel Generator." https://apelectric.com/winco-dr500f4-500kw-diesel-generator/ (accessed Dec. 1, 2020.

[34] "Climate South El Monte." https://www.meteoblue.com/en/weather/historyclimate/climatemodelled/south-el-monte_united-states-of-america_5397376 (accessed Dec. 1, 2020, 2020).

[35] D. W. Hart, *Power Electronics*. New York, NY: McGraw-Hill Companies, Inc., 2010.

[36] R. Dahanayake. "3 Phase Inverter." https://www.mathworks.com/matlabcentral/fileexchange/44676-3-phase-inverter (accessed 2021/01/03.

[37] "Getting Started with Stateflow Video." https://www.mathworks.com/videos/getting-started-with-stateflow-1608719415568.html (accessed 2021/01/17.

[38] "Finite State Machines / Flow Designer." https://qoretechnologies.com/manual/qorus/current/qorus/finite_state_machines.html (accessed.

[39] G. Warren *et al.* "State Machine Workflows." https://docs.microsoft.com/en-us/dotnet/framework/windows-workflow-foundation/state-machine-workflows (accessed 2021/01/23.